Secondary organic aerosol from chlorine-initiated oxidation of isoprene

Dongyu S. Wang and Lea Hildebrandt Ruiz

McKetta Department of Chemical Engineering, The University of Texas at Austin, Austin, TX 78756, USA

5 *Correspondence to*: Lea Hildebrandt Ruiz (lhr@che.utexas.edu)

Abstract. Recent studies have found inland concentrations of reactive chlorine species to be higher than expected, suggesting that atmospheric chlorine chemistry is more extensive than previously thought. Chlorine radicals can interact with HO_x radicals and nitrogen oxides (NO_x) to alter the oxidative capacity of the atmosphere. They are known to rapidly oxidize a wide range of volatile organic compounds (VOC) found in the atmosphere, yet little is known about secondary organic aerosol (SOA)

10 formation from chlorine-initiated photo-oxidation and its atmospheric implications. Environmental chamber experiments were carried out under low-NO_x conditions with isoprene and chlorine as primary VOC and oxidant sources. Upon complete isoprene consumption, observed SOA yields ranged from 8 % to 36 %, decreasing with extended photo-oxidation and SOA aging. A High-Resolution Time-of-Flight Chemical Ionization Mass Spectrometer was used to determine the molecular composition of gas-phase species using iodide-water and hydronium-water ionization. Ions consistent with isoprene-derived

15 epoxydiol (IEPOX) and other common OH-isoprene oxidation products were observed, evident of secondary OH production and resulting chemistry from Cl-initiated reactions.

1 Introduction

Studies have shown that long-term exposure to fine particulate matter (PM), also known as aerosol, is linked to increases in mortality and cardiorespiratory diseases (Dockery et al., 1993; Pope et al., 2006). Short term exposure to aerosol could also

20 induce stress response and cytotoxicity in cells (de Bruijne et al., 2009; Ebersviller et al., 2012; Hawley et al., 2014). Equilibrium partitioning of oxidized, semi-volatile organic compounds (Pankow, 1994), collectively referred to as secondary organic aerosol (SOA), contributes 20–90 % to the global fine aerosol budget (Jimenez et al., 2009; Kanakidou et al., 2005). The majority of SOA originates from oxidation of biogenic volatile organic compounds (BVOCs), which account for ~90% of annual non-methane hydrocarbon emissions (Goldstein and Galbally, 2007; Guenther et al., 2012), among which isoprene

25 has the highest emission rate at ~600 Tg/yr (Guenther et al., 2006). Isoprene SOA formation initiated by ozone, hydroxyl, and nitrate radicals has been studied extensively and is estimated to account for 6–30 Tg/yr of the global aerosol budget (Brégonzio-Rozier et al., 2015; Claeys, 2004; Guenther et al., 2006; Kroll et al., 2006; Lin et al., 2012; Surratt et al., 2006, 2010; Zhao et al., 2015). Meanwhile, little is known about SOA from chlorine-initiated oxidation of isoprene.

The concentration of chlorine radicals is approximately one order of magnitude lower compared to OH radicals under ambient conditions (Faxon and Allen, 2013), but due to its high reactivity towards numerous VOCs, chlorine radicals could contribute significantly as a primary oxidant under certain circumstances (Riedel et al., 2012; Riva et al., 2015; Young et al., 2014). Hydrogen-abstraction and chlorine-addition to alkenes produce peroxy and chloroperoxy radicals, respectively, that

5   could lead to formation of semi-volatile oxidized products. Studies have shown that chlorine-initiated oxidation of alpha-pinene (Cai and Griffin, 2006; Ofner et al., 2013), toluene (Cai et al., 2008; Huang et al., 2014; Karlsson et al., 2001), and polycyclic aromatic hydrocarbons (PAHs, Riva et al., 2015) lead to SOA formation, with close to unity SOA yield reported for select PAHs (Riva et al., 2015). Reactive chlorine species could also enhance OH-radical propagation (Young et al., 2014), nocturnal NO_x recycling (Riedel et al., 2012; Thornton et al., 2010), and ozone production (Tanaka et al., 2003), further

10   increasing the oxidative capacity of the atmosphere. Recent studies show that air quality models severely under-predict the abundance of inland reactive chlorine species (Faxon and Allen, 2013; Faxon et al., 2015; Riedel et al., 2012; Thornton et al., 2010), suggesting that chlorine chemistry may be more extensive than previously thought.

Chlorine-initiated oxidation of isoprene could either proceed via the dominant (85 %) chlorine addition pathway, much like OH-isoprene reactions, or proceed via a minor (15 %) hydrogen-abstraction pathway (Fantechi et al., 1998; Lei and Zhang,

15   2000; Nordmeyer et al., 1997; Orlando et al., 2003). Major gas-phase products include methyl vinyl ketone (MVK), methacrolein (MACR), chloroacetone, chloroacetaldehyde, hydrochloric acid, and isomers of 3-methyl-3-butene-2-one (CMBO), a unique tracer for atmospheric chlorine chemistry (Nordmeyer et al., 1997; Riemer et al., 2008; Tanaka et al., 2003). The rate constant of the isoprene-chlorine reaction at 25°C (2.64–5.50×10^{-10} molecules^{-1} cm^3) (Fantechi et al., 1998; Orlando et al., 2003; Ragains and FinlaysonPitts, 1997) is much faster than the rate constant of the isoprene-OH reaction (1.00×10^{-10}

20   molecules^{-1} cm^3) (Atkinson and Arey, 2003), suggesting that isoprene-chlorine chemistry could compete with isoprene-OH chemistry under certain conditions. Moreover, reactions between chlorine and isoprene or isoprene-derived SOA could serve as a reactive chlorine sink in the atmosphere, as has been proposed for reactions between chlorine and biogenic SOA (Ofner et al., 2012). To our knowledge, SOA formation from chlorine-initiated oxidation of isoprene has not been reported in literature. To address this significant knowledge gap, we conducted environmental chamber studies using chlorine radicals as

25   the primary oxidant source for isoprene oxidation under low NO_x conditions, which could dominate in remote coastal regions. We report SOA composition, yields and select gas-phase products.

2 Methods

2.1 Environmental Chamber Experiments

Experiments were performed at 25° C under low relative humidity (RH < 10%) and low NO_x (<5 ppb) conditions in a 12 m^3

30   temperature-controlled Teflon® chamber lined with UVA lights. Chamber characteristics were described elsewhere (Bean and Hildebrandt Ruiz, 2016). Temperature, RH, concentration of ozone, NO, NO_2, and NO_x were continuously monitored. The chamber was flushed with dry clean air at a flowrate exceeding100 liters per minute (LPM) for at least 12 hours before each

experiment. Between experiments, "blank experiments" were conducted in which seed particles, ozone, and chlorine gas (Cl_2 Airgas, 106 ppm in N_2) were injected into the chamber at high concentrations and UV lights were turned on to remove any residual organics.

For each experiment, microliters of isoprene (Acros Organics, 98% stabilized) were transferred into a glass sampling tube (Kimble-Chase, 250 ml), which was then flushed with zero air into the chamber. Two Cl_2 injection methods were used: For "initial case" experiments, all Cl_2 was injected in the dark and allowed to mix with isoprene prior to photo-oxidation. For "continuous case" experiments, Cl_2 was injected continuously with UV lights on at 0.1 LPM with an additional 0.9 LPM clean air dilution flow, equivalent to ~0.88 ppb/min Cl_2 into the chamber. Depositional particle wall loss was constrained using dried, monomodal, and polydisperse ammonium sulfate seed particles introduced prior to photo-oxidation.

2.2 Instrumentation

A High-Resolution Time-of-Flight Chemical Ionization Mass Spectrometer (Aerodyne Research Inc., "CIMS") was used to measure gas-phase organic compounds via proton transfer, charge exchange, or clustering with chemical ionization (CI) reagent ions, with humidified ultra-high purity nitrogen as the carrier gas. Hydronium-water cluster ($[H_2O]_nH_3O^+$) ionization detected isoprene and select moderately oxidized species. Iodide-water cluster ($[H_2O]_nI^-$) ionization detected select highly oxidized and acidic species (Aljawhary et al., 2013; Lee et al., 2014). Detailed theory and operation of the CIMS are discussed elsewhere (Aljawhary et al., 2013; Bertram et al., 2011; Lee et al., 2014; Yatavelli et al., 2012).

An Aerosol Chemical Speciation Monitor (Aerodyne Research Inc., "ACSM") was used to determine the bulk chemical composition of submicron, non-refractory aerosol species (Ng et al., 2011). Analytes are flash-vaporized at 600° C, ionized via electron impact ionization (EI) (Ng et al., 2011), and then measured by a quadrupole mass spectrometer. Background-corrected ("difference") mass spectra are obtained by subtracting filtered ("closed") from unfiltered ("open") measurements (Ng et al., 2011). A standard fragmentation table is used to speciate difference mass spectra (Allan et al., 2004). Calibration is performed with 300 nm size-selected ammonium nitrate and ammonium sulfate aerosol to determine the response factor for particulate nitrate and the relatively ionization efficiencies (RIE) for sulfate and ammonium; these values are needed to convert ion intensities to mass concentrations (Ng et al., 2011). Particle volume and size distributions were measured using a Scanning Electrical Mobility Spectrometer (Brechtel, SEMS Model 2002) consisting of a Differential Mobility Analyzer and a butanol Condensation Particle Counter. SEMS sheath and sample flowrates were set to 5 and 0.35 LPM, respectively, covering a 10–1000 nm sizing range.

2.3 Data Analysis

Suspended particles are lost to the Teflon® chamber wall over time, for which numerous correction methods have been proposed (Carter et al., 2005; Hildebrandt et al., 2009; Ng et al., 2007; Pathak et al., 2007; Pierce et al., 2008; Verheggen and Mozurkewich, 2006). Recent studies also report loss of organic vapors to Teflon surfaces (Kokkola et al., 2014; Krechmer et al., 2016; Loza et al., 2010; Matsunaga and Ziemann, 2010; Zhang et al., 2015). Assuming internal mixing of particles and

that organic vapor can condense onto suspended and wall-deposited particles alike, we corrected for particle wall loss and the loss of organic vapors onto wall-deposited particles using the organic-to-sulfate ratio (Hildebrandt et al., 2009),

$$C_{OA}(t) = \frac{C_{OA}^{sus}(t)}{C_{seed}^{sus}(t)} C_{seed}^{sus}(t = 0) , \tag{1}$$

where $C_{OA}^{sus}(t)$ is the suspended organic aerosol (OA) concentration, which was zero at the start of each experiment, $C_{seed}^{sus}(t)$

5 is the suspended ammonium sulfate seed particle concentration, $C_{seed}^{sus}(t = 0)$ is the suspended seed particle mass concentration at the start of photo-oxidation, and $C_{OA}(t)$ is the corrected OA concentration. Note that Eq. (1) does not account for loss of organic vapors to clean Teflon surfaces, which could be significant for SVOCs (Krechmer et al., 2016).

SOA yield, Y, is calculated as,

$$Y = \frac{C_{OA}}{\Delta VOC} , \tag{2}$$

10 where ΔVOC is the amount of VOC consumed. Based on absorptive equilibrium partitioning theory (Odum Jay et al., 1996; Pankow, 1994), the volatility basis set (VBS) framework (Donahue et al., 2006) states that

$$Y = \xi = \sum_i \alpha_i \xi_i ; \; C_i = \alpha_i \Delta VOC; \; \xi_i = \left(1 + \frac{C_i^*}{C_{OA}}\right)^{-1} ; \; C_{OA} = \sum_i C_i \xi_i , \tag{3}$$

where C_i^* is the effective saturation concentration of the surrogate compound in VBS bin i in µg m^{-3}; α_i, C_i, ξ_i are the total yield, total mass concentration, and the condensed phase mass fraction of bin i, respectively. By rearranging Eq. (3), we can

15 derive an expression for the minimum VOC consumption required for SOA formation (see section S1),

$$(\Delta VOC_{min})^{-1} = \sum_1^n \frac{\alpha_i}{C_i^*} , \tag{4}$$

where ΔVOC_{min} is low if low-volatility compounds dominate the aerosol phase. When aerosol volatility is low and aerosol loading is high, the condensed phase mass fraction approaches 1, where the "maximum" SOA yield (Griffin et al., 1999) according to Eq. (2) and Eq. (3) is

20 $$Y_{max} = \sum_1^n \alpha_i \tag{5}$$

The extent of SOA oxidation is often depicted using f_{44} and f_{43}, which represent the fractional contribution to the total organic ion signal from ion fragments at mass-to-charge (m/z) 44 (mostly CO_2^+, a proxy for doubly-oxidized compounds) and at m/z 43 (mostly $C_2H_3O^+$, a proxy for singly-oxidized compounds), respectively (Chan et al., 2010; Chhabra et al., 2011). Based on empirical correlations, the oxygen-to-carbon ratio (O:C), the hydrogen-to-carbon ratio (H:C), and the oxidation state

of carbon ($\overline{OS_c}$) can be estimated from f_{44} alone as summarized in section S2 (Canagaratna et al., 2015; Donahue et al., 2012; Heald et al., 2010; Kroll et al., 2011).

High resolution mass spectra fitting of CIMS data was performed using the software Tofware V2.5.7 (Tofwerk) in Igor Pro V6.37 (Wavemetrics Inc.). CIMS sensitivity correction utilized the Active Chemical Ionization Mass Spectroscopy (ACIMS) formula (de Gouw and Warneke, 2007), normalizing all product ion signals against dominant reagent ion signals, $[H_2O]_nH_3O^+$ and $[H_2O]_nI^-$. For most experiments conducted, the reagent signals were at least five times greater than the summed product signals, equivalent to less than 10 % overcorrection by ACIMS compared to more rigorous methods such as Parallel-ACIMS, which accounts for reagent ion depletion (see section S3 for a more detailed discussion). Because the CIMS cannot distinguish between isomers and because of the lack of calibration standards, gas-phase data presented here are normalized by the maximum signals for qualitative interpretations only.

3 Results and Discussion

3.1 SOA Formation, Ageing, and Composition

Table 1 summarizes the experimental conditions and results. Figure 1 compares wall loss-corrected SOA time series from two experiments with similar precursor concentrations. In the continuous chlorine experiment (C2), isoprene gradually reacted away during chlorine injection; SOA concentration steadily increased until isoprene was depleted, at which point SOA concentration began to decay, likely due to vapor wall loss (Boyd et al., 2015; Krechmer et al., 2016) and oxidative fragmentation (Kroll et al., 2011). The initial chlorine experiment (A4) exhibited similar trends, though the initial SOA decay rate was very fast, likely due to rapid oxidation and fragmentation of reaction products, and loss of early generation low-volatility products that are especially susceptible towards vapor wall loss effects (Boyd et al., 2015). It should be noted that little SOA formation delay was observed in all experiments. ΔVOC_{min} from Eq. (4) is therefore small, suggesting that the initial oxidation products responsible for SOA formation have very low volatility. Prompt SOA formation was also observed in previous work for chlorine-initiated oxidation of α-pinene (Ofner et al., 2013), as well as for chlorine-initiated homogenous nucleation of toluene SOA (Huang et al., 2012). Formation of low volatility early generation products may be a common feature of chlorine-initiated oxidation. Outside of the initial period, some vapor wall loss was observed, although oxidative fragmentation appeared to be the main cause of SOA mass decrease (see section S2 and Fig. S1).

Figure 2 shows that SOA oxidation state, represented by f_{44}, depended on the initial isoprene concentration and was unaffected by the oxidant injection method. Because isoprene is more reactive towards chlorine radicals than its oxidation products, such as MVK and MACR (Orlando et al., 2003), isoprene could scavenge radicals and delay SOA aging. Additionally, increased OA mass loading could absorb less oxidized and more volatile compounds into the particle-phase, lowering the observed SOA oxidation state at higher initial isoprene concentrations. Estimated $\overline{OS_c}$ of chlorine-isoprene SOA increased from -0.5 to over 1 during experiment C1, characteristic of the evolution of semi-volatile oxygenated OA (SV-OOA) to low-volatility oxygenated OA (LV-OOA) (Kroll et al., 2011). Oxidation of chlorine-isoprene SOA formed under low NOₓ

follows a similar trajectory as OH-isoprene SOA formed under higher NO_x, which is considerably more oxidized than OH-isoprene SOA formed under low NO_x (Chhabra et al., 2011), as shown in Figure 3. The oxidizing capacity of chlorine radicals has also been demonstrated for select biogenic SOA derived from α-pinene, catechol, and guaiacol, where halogenation led to significant SOA aging, formation of high molecular weight compounds, and particle growth (Ofner et al., 2012). High

5   reactivity of chlorine radicals towards isoprene and its reaction products meant that extensive SOA processing could be easily achieved within laboratory timescales.

3.2 Particulate Organic Chloride

Chlorine addition to the double bond is the dominant (~85%) isoprene-chlorine reaction pathway (Fan and Zhang, 2004; Ragains and FinlaysonPitts, 1997). Formation of semi-volatile and low-volatility chlorinated organic compounds could be

10   expected, but quantification proved to be difficult. As shown in Fig. 4 for Exp. H1, significant particulate chloride formation (over 9 % of total SOA mass) was initially observed, which then decreased to near background levels. In other experiments, particulate chloride concentrations were near the detection limit. The low measured chloride concentration was likely due to incomplete vaporization of chlorinated compounds during the sample ("open") period, resulting in particulate matter vaporization during the filter ("closed") period and overestimation of background signals. Furthermore, our analysis shows

15   that while the difference signal of a fast-desorbing chloride ion fragment (HCl^+) correlates well with OA, the difference signal of a slow-desorbing ion fragment (Cl^+) anti-correlates with OA (Fig. S7). The background Cl^+ signal was consistently higher than the sample Cl^+ signal, except when the sample chloride concentration increased significantly faster than background, as was the case for Exp. H1, a high-concentration experiment. Our results show that the particulate chloride observed was likely organic chloride. The presence of organic chloride aerosol has been observed previously in SOA from chlorine-initiated

20   oxidation of α-pinene (Ofner et al., 2013), in SOA which was post processed by halogenation (Ofner et al., 2012), as well as in new particle formation from 1,8-cineol and limonene over simulated salt lakes (Kamilli et al., 2015) using ion cyclotron-Fourier transform/mass spectroscopy. To date, this is the only reported study of organic chloride measurement using an ACSM. A more detailed discussion of organic chloride detection with the ACSM can be found in section S4.

Low abundance has been cited as the reason for highly variable measurements of ambient chloride using ACSM and similar

25   instruments (Crenn et al., 2015). Overall, our results indicate that the standard operating procedure of the ACSM and similar instrumentation may systematically underestimate chloride concentration. To better quantify chloride, the filtered measurement period could be extended to better capture the true background. Higher vaporizer temperatures could be applied to desorb low-volatility species more efficiently, but doing so could also change the fragmentation profile. Another idea would be to only use fast-desorbing chloride (HCl^+ ions) for quantification: For SOA from chlorine-initiated oxidation of isoprene

30   under low NO_x, the average (HCl^+)-to-organics ratio was 0.072 ± 0.009 (Fig. S8).

3.3 SOA Yield

It is customary to present SOA yield as a function of OA loading. From Eq. (2), when the VOC precursor has been depleted, all subsequent yield Y varies linearly with C_{OA} along a slope of $(\Delta VOC_0)^{-1}$, the inverse of the initial VOC concentration. Post VOC depletion, SOA mass may further increase as multi-generation oxidation products partition to the particle phase, but

5   SOA mass will eventually decrease due to fragmentation (Kroll et al., 2011). In theory, all VOC-oxidant mixtures whose ΔVOC_{min} is less than VOC_0 eventually fall somewhere on the same, pre-defined yield "line" with slope $(\Delta VOC_0)^{-1}$, and will converge (to Cartesian origin) over time as fragmentation becomes dominant. This pre-defined yield curve is thus non-unique and depends only on VOC_0. Incorporating data collected after VOC depletion, whether from the same experiment or different experiments with similar initial VOC_0 values, biases the VBS fitting parameters towards the pre-defined yield curve (see

10   section S5). Therefore, 1-dimensional VBS fitting is not sufficient to describe SOA formation and oxidation post VOC depletion, as numerous studies have also pointed out (Kroll et al., 2007; Liu et al., 2016; Xu et al., 2014). A two-dimensional model would be more appropriate in these cases (Chuang and Donahue, 2016; Donahue et al., 2012; Murphy et al., 2012).

Considering the different oxidation conditions examined in this study, varying initial isoprene concentration, chlorine concentration, and duration of oxidation, we did not perform 1-D VBS fitting on the collective dataset. Instead, the highest

15   observed SOA yields from each experiment are reported in Table 1 and compared with literature values (Brégonzio-Rozier et al., 2015; Koo et al., 2014; Liu et al., 2016; Xu et al., 2014) in Fig. 5. Maximum SOA yields were lower for continuous cases, likely because there was less suspended absorbing mass to retain initial low-volatility products or to compete with vapor wall loss. It also took longer for continuous cases to reach maximum SOA concentrations, as shown in Fig. 1; the effects of vapor wall loss and oxidative fragmentation seemed to be more pronounced. Highest SOA yields observed for initial cases (A2–A5)

20   were on average 23.7 ± 3.5 %. For continuous cases (C1–C4), the average was 9.5 ± 1.3 %, similar to yields reported for OH-oxidation by recent publications (Liu et al., 2016; Xu et al., 2014). Recall that the f_{44} vs f_{43} patterns observed were also similar for chlorine-isoprene and OH-isoprene SOA, as shown in Fig. 3. This suggests that OH- and chlorine-initiated oxidation of isoprene may result in SOA of similar bulk vapor pressure and oxidation state. This is also suggested by gas-phase measurements as explained below.

25   ### 3.4 Gas-phase products: Overlaps with OH chemistry

Using $(H_2O)_nH_3O^+$ CIMS, we observed ions consistent with isoprene [$C_5H_8^+$ and $(C_5H_8)H^+$], methacrolein (MACR)/methyl vinyl ketone (MVK) [$(C_4H_6O)H^+$], isomers of 3-methyl-3-butene-2-one ("CMBO") [$(C_5H_7OCl)H^+$], chloroacetone [$(C_3H_5OCl)H^+$], and other gas-phase oxidation products, as shown in Fig. 6. CMBO and MVK/MACR were among the earliest oxidation products, which were likely further oxidized to produce SOA, as shown in Figure 6a. MVK and MACR are also key

30   intermediary products in OH-isoprene reactions from $NO + RO_2$ and $RO_2 + RO_2$ reaction pathways (Kroll et al., 2006), where MACR is a known SOA precursor (Brégonzio-Rozier et al., 2015; Xu et al., 2014), which could contribute to some similarities between OH-isoprene and chlorine-isoprene SOA. Multiple generations of chlorinated C_5 compounds were also observed in

the gas-phase, as shown in Fig. 6a and 7a, possibly from continued oxidation of CMBO and chlorination of 2-methyl-3-buten-2-ol (MBO), which further demonstrates that semi-volatile and low volatility organic chlorides should be present. CMBO has long been identified as a unique gas-phase marker for isoprene-chlorine oxidation (Nordmeyer et al., 1997; Riemer et al., 2008; Tanaka et al., 2003). Degradation of CMBO by OH is implemented in some air quality models, though only with inferred

5   reaction rates (Tanaka and Allen, 2001). The degradation of CMBO and its role as a potential SOA precursor could have important implications for estimating atmospheric chlorine activity and warrant future investigation.

The formation of CMBO also produces HO_2 hydroperoxy radicals (Orlando et al., 2003; Ragains and FinlaysonPitts, 1997), serving as a source of secondary OH radicals. Other unidentified HO_x production pathways could also be present. Evidence of secondary OH radical production has been reported for NO_3-oxidation of isoprene (Kwan et al., 2012; Schwantes et al., 2015),

10   for chlorine-initiated oxidation of methylnaphthalenes and naphthalene under low-NO_x (Riva et al., 2015; Wang et al., 2005) and for chlorine-initiated oxidation of toluene under high NO_x (Huang et al., 2012). Figure 7a shows the accumulation of ClOH observed using $(H_2O)I^-$ CIMS during the SOA growth period, where HO_x radicals produced from chlorine-isoprene oxidation could react with excess chlorine. Production of OH is also possible from reactions between NO and HO_2 radicals, which would be more pronounced under high NO_x conditions. No NO_x was added to our experiments, and measured concentrations were

15   below 5 ppb, mostly in the form of NO_2. Because isoprene is not detected using $(H_2O)I^-$ CIMS, we use the SOA trend as a common reference. It can be seen in Fig. 1 and 6a that isoprene depletion roughly coincides with the SOA concentration peak. This explains the reversal from ClOH production to ClOH decay following the SOA concentration peak shown in Fig. 7a, when HO_x radical production from isoprene-chlorine oxidation (e.g. formation of CMBO) ceased due to isoprene depletion. Accumulated ClOH was then gradually photolyzed under UV. In the absence of a primary oxidant source, such as when

20   chlorine injection stopped in Exp. C3, ClOH could provide residual OH and chlorine radicals under UV, as shown in Fig. 7a. Under dark, dry, and low-NO_x conditions, ClOH remains stable as a temporary radical reservoir, as shown in Fig. 7a during the period when UV lights were turned off.

Secondary OH chemistry may have also contributed to SOA formation. Ions consistent with isoprene-derived hydroxyl hydroperoxides (ISOPOOH) or isoprene-derived epoxydiols (IEPOX) were observed in both CIMS modes, as shown in Fig.

25   6b and 7b. Reactive uptake and oxidation of IEPOX has been reported to contribute significantly to SOA mass during isoprene OH-oxidation (Bates et al., 2014; Paulot et al., 2009; Surratt et al., 2010), especially under acidic or humid conditions (Lewandowski et al., 2015; Nguyen et al., 2014). Figure 6b shows that $(C_5H_{10}O_3)H^+$ ions correlated well with SOA growth. However, there are several ways to produce $(C_5H_{10}O_3)H^+$ ions in addition to direct protonation, such as clustering or ligand exchange between $C_5H_8O_2$ (e.g. methyl methacrylate) and $(H_2O)_nH_3O^+$ reagent ions, as well as fragmentation of

30     $(C_5H_{11}O_3Cl)H^+$ product ions. As seen in Fig. 6b, the qualitative $(C_5H_{10}O_3)H^+$ trend is similar to that of both $(C_5H_8O_2)H^+$ and $(C_5H_{11}O_3Cl)H^+$. Furthermore, ions that would be consistent with IEPOX-oxidation products, such as $(C_5H_8O_3)H^+$ were observed to precede the formation of $(C_5H_{10}O_3)H^+$. In contrast, $(H_2O)I^-$ CIMS measurements show distinct trends for $C_5H_{10}O_3$ (detected as $[(C_5H_{10}O_3)I^-]$) and $C_5H_8O_2$ (detected as $[(C_5H_8O_2)I^-]$) in Fig. 7b. While $(C_5H_8O_2)I^-$ correlated well with SOA growth and decay, as $(C_5H_8O_2)H^+$ and $(C_5H_{10}O_3)H^+$ did in Fig. 6a, $(C_5H_{10}O_3)I^-$ resembled an intermediary species and a SOA

precursor, consistent with the role of IEPOX during OH-oxidation of isoprene. This suggests that IEPOX was observed only with $(H_2O)I^-$ CIMS while its oxidation products were observed by both $(H_2O)_nH_3O^+$ and $(H_2O)I^-$ CIMS. Without any information on the chemical structure, it is also possible that $(C_5H_{10}O_3)I^-$ is the fragment of some unidentified parent ion(s) or that it is an IEPOX isomer produced form non-OH-reaction pathways. Moreover, photooxidative degradation of chlorinated

5   organic compounds could produce products that resemble OH-oxidation products like $C_5H_{10}O_3$. A similar observation has been reported for chlorine-initiation oxidation of α-pinene, where the SOA appeared less like halogenated organic aerosols as oxidation continued (Ofner et al., 2013). Regardless, it is evident that SOA formation from chlorine-initiated and OH-initiated oxidation of isoprene proceeds via multi-generational oxidation chemistries involving similar, if not identical, key gas-phase products.

10   **4 Conclusions**

Chlorine-initiated oxidation of isoprene under low NO_x was investigated inside an environmental chamber. Chlorine was injected either in bulk or continuously in low amounts to simulate fast and slow oxidation conditions; prompt SOA formation was observed in both cases, indicative of low volatility initial product formation. Average wall loss-corrected SOA yield was 9.5 ± 1.3 % for continuous chlorine injection experiments and 23.7 ± 3.5 % for initial injection experiments; the differences

15   resulted from loss of initial low volatility products and organic vapor to the chamber wall, and from oxidative fragmentation of SOA. 1-D VBS fitting should not include yield data collected post VOC depletion. The effects of SOA aging must be described explicitly and separately from initial SOA formation.

The extent of SOA oxidation was similar to that of SOA formed from OH-oxidation of isoprene under high NO_x reported in the literature. Chloride fragments at *m/z* 35 were found to desorb slowly and to interfere with chloride quantification using

20   standard operating and data analysis procedures. We propose alternative methods for improved organic chloride quantification including extended filter sampling and the use of "fast" desorbing chloride fragments (at *m/z* 36) for quantifying chloride, which accounted for approximately 6.7 % of total SOA mass in these experiments. Measurements by HR-ToF-CIMS show evidence of chlorine-initiated secondary OH chemistry and continued oxidation of gas-phase products by chlorine and OH radicals.

25   SOA formation from chlorine-initiated oxidation of isoprene is reported for the first time. The high isoprene-chlorine SOA yields suggest that, despite comparatively low ambient abundance, chlorine radicals could have a notable contribution to overall SOA formation. The chlorine-addition dominated oxidation pathway, presence of particulate chloride, and difficulties associated with particulate chloride quantification suggest that the prevalence of particulate organic chloride in the ambient atmosphere is likely underestimated. Similarities between chlorine-isoprene and OH-isoprene oxidation products suggest that

30   air quality models may be able to lump the treatment of SOA produced from chlorine- and OH- initiated oxidation of isoprene.

Acknowledgements

This material is based upon work supported by the National Science Foundation under Grant No. 1653625. The work was also funded in part with funds from the State of Texas as part of the program of the Texas Air Research Center. The contents do not necessarily reflect the views and policies of the sponsor nor does the mention of trade names or commercial products
5   constitute endorsement or recommendation for use.

References

Aljawhary, D., Lee, a. K. Y. and Abbatt, J. P. D.: High-resolution chemical ionization mass spectrometry (ToF-CIMS): Application to study SOA composition and processing, Atmos. Meas. Tech., 6(11), 3211–3224, doi:10.5194/amt-6-3211-2013, 2013.

10   Allan, J. D., Delia, A. E., Coe, H., Bower, K. N., Alfarra, M. R., Jimenez, J. L., Middlebrook, A. M., Drewnick, F., Onasch, T. B., Canagaratna, M. R., Jayne, J. T. and Worsnop, D. R.: A generalised method for the extraction of chemically resolved mass spectra from Aerodyne aerosol mass spectrometer data, J. Aerosol Sci., 35(7), 909–922, doi:10.1016/j.jaerosci.2004.02.007, 2004.

Atkinson, R. and Arey, J.: Atmospheric Degradation of Volatile Organic Compounds, Chem. Rev., 103(12), 4605–4638,
15   doi:10.1021/cr0206420, 2003.

Bates, K. H., Crounse, J. D., St. Clair, J. M., Bennett, N. B., Nguyen, T. B., Seinfeld, J. H., Stoltz, B. M. and Wennberg, P. O.: Gas phase production and loss of isoprene epoxydiols, J. Phys. Chem. A, 118(7), 1237–1246, doi:10.1021/jp4107958, 2014.

Bean, J. and Hildebrandt Ruiz, L.: Hydrolysis and Gas-particle Partitioning of Organic Nitrates Formed in Environmental
20   Chamber Experiments, Atmos. Chem. Phys., in press, 2016.

Bertram, T. H., Kimmel, J. R., Crisp, T. A., Ryder, O. S., Yatavelli, R. L. N., Thornton, J. A., Cubison, M. J., Gonin, M. and Worsnop, D. R.: A field-deployable, chemical ionization time-of-flight mass spectrometer, Atmos. Meas. Tech., 4(7), 1471–1479, doi:10.5194/amt-4-1471-2011, 2011.

Boyd, C. M., Sanchez, J., Xu, L., Eugene, a. J., Nah, T., Tuet, W. Y., Guzman, M. I. and Ng, N. L.: Secondary organic aerosol
25   formation from the β-pinene+NO₃ system: effect of humidity and peroxy radical fate, Atmos. Chem. Phys., 15(13), 7497–7522, doi:10.5194/acp-15-7497-2015, 2015.

Brégonzio-Rozier, L., Siekmann, F., Giorio, C., Pangui, E., Morales, S. B., Temime-Roussel, B., Gratien, A., Michoud, V., Ravier, S., Cazaunau, M., Tapparo, A., Monod, A. and Doussin, J. F.: Gaseous products and secondary organic aerosol formation during long term oxidation of isoprene and methacrolein, Atmos. Chem. Phys., 15(6), 2953–2968,
30   doi:10.5194/acp-15-2953-2015, 2015.

de Bruijne, K., Ebersviller, S., Sexton, K. G., Lake, S., Leith, D., Goodman, R., Jetters, J., Walters, G. W., Doyle-Eisele, M., Woodside, R., Jeffries, H. E. and Jaspers, I.: Design and testing of Electrostatic Aerosol in Vitro Exposure System

(EAVES): an alternative exposure system for particles., Inhal. Toxicol., 21(2), 91–101, doi:10.1080/08958370802166035, 2009.

Cai, X. and Griffin, R. J.: Secondary aerosol formation from the oxidation of biogenic hydrocarbons by chlorine atoms, J. Geophys. Res. Atmos., 111(14), 7348–7359, doi:10.1029/2005JD006857, 2006.

Cai, X., Ziemba, L. D. and Griffin, R. J.: Secondary aerosol formation from the oxidation of toluene by chlorine atoms, Atmos. Environ., 42(32), 7348–7359, doi:10.1016/j.atmosenv.2008.07.014, 2008.

Canagaratna, M. R., Jimenez, J. L., Kroll, J. H., Chen, Q., Kessler, S. H., Massoli, P., Hildebrandt Ruiz, L., Fortner, E., Williams, L. R., Wilson, K. R., Surratt, J. D., Donahue, N. M., Jayne, J. T. and Worsnop, D. R.: Elemental ratio measurements of organic compounds using aerosol mass spectrometry: Characterization, improved calibration, and implications, Atmos. Chem. Phys., 15(1), 253–272, doi:10.5194/acp-15-253-2015, 2015.

Carter, W. P. L., Cocker, D. R., Fitz, D. R., Malkina, I. L., Bumiller, K., Sauer, C. G., Pisano, J. T., Bufalino, C. and Song, C.: A new environmental chamber for evaluation of gas-phase chemical mechanisms and secondary aerosol formation, Atmos. Environ., 39(40), 7768–7788, doi:10.1016/j.atmosenv.2005.08.040, 2005.

Chan, M. N., Surratt, J. D., Claeys, M., Edgerton, E. S., Tanner, R. L., Shaw, S. L., Zheng, M., Knipping, E. M., Eddingsaas, N. C., Wennberg, P. O. and Seinfeld, J. H.: Characterization and quantification of isoprene-derived epoxydiols in ambient aerosol in the southeastern united states, Environ. Sci. Technol., 44(12), 4590–4596, doi:10.1021/es100596b, 2010.

Chhabra, P. S., Ng, N. L., Canagaratna, M. R., Corrigan, A. L., Russell, L. M., Worsnop, D. R., Flagan, R. C. and Seinfeld, J. H.: Elemental composition and oxidation of chamber organic aerosol, Atmos. Chem. Phys., 11(17), 8827–8845, doi:10.5194/acp-11-8827-2011, 2011.

Chuang, W. K. and Donahue, N. M.: A two-dimensional volatility basis set – Part 3: Prognostic modeling and NO$_x$ dependence, Atmos. Chem. Phys., 16(1), 123–134, doi:10.5194/acp-16-123-2016, 2016.

Claeys, M.: Formation of Secondary Organic Aerosols Through Photooxidation of Isoprene, Science (80-.)., 303(5661), 1173–1176, doi:10.1126/science.1092805, 2004.

Crenn, V., Sciare, J., Croteau, P. L., Verlhac, S., Fröhlich, R., Belis, C. A., Aas, W., Äijälä, M., Alastuey, A., Artiñano, B., Baisnée, D., Bonnaire, N., Bressi, M., Canagaratna, M., Canonaco, F., Carbone, C., Cavalli, F., Coz, E., Cubison, M. J., Esser-Gietl, J. K., Green, D. C., Gros, V., Heikkinen, L., Herrmann, H., Lunder, C., Minguillón, M. C., Močnik, G., O'Dowd, C. D., Ovadnevaite, J., Petit, J. E., Petralia, E., Poulain, L., Priestman, M., Riffault, V., Ripoll, A., Sarda-Estève, R., Slowik, J. G., Setyan, A., Wiedensohler, A., Baltensperger, U., Prévôt, A. S. H., Jayne, J. T. and Favez, O.: ACTRIS ACSM intercomparison - Part 1: Reproducibility of concentration and fragment results from 13 individual Quadrupole Aerosol Chemical Speciation Monitors (Q-ACSM) and consistency with co-located instruments, Atmos. Meas. Tech., 8(12), 5063–5087, doi:10.5194/amt-8-5063-2015, 2015.

Dockery, D. W., Pope, C. A., Xu, X., Spengler, J. D., Ware, J. H., Fay, M. E., Ferris, B. G. and Speizer, F. E.: An Association between Air Pollution and Mortality in Six U.S. Cities, N. Engl. J. Med., 329(24), 1753–1759, doi:10.1056/NEJM199312093292401, 1993.

Donahue, N. M., Robinson, A. L., Stanier, C. O. and Pandis, S. N.: Coupled partitioning, dilution, and chemical aging of semivolatile organics, Environ. Sci. Technol., 40(8), 2635–2643, doi:10.1021/es052297c, 2006.

Donahue, N. M., Kroll, J. H., Pandis, S. N. and Robinson, A. L.: A two-dimensional volatility basis set-Part 2: Diagnostics of organic-aerosol evolution, Atmos. Chem. Phys., 12(2), 615–634, doi:10.5194/acp-12-615-2012, 2012.

5 Ebersviller, S., Lichtveld, K., Sexton, K. G., Zavala, J., Lin, Y.-H., Jaspers, I. and Jeffries, H. E.: Gaseous VOCs rapidly modify particulate matter and its biological effects - Part 1: Simple VOCs and model PM, Atmos. Chem. Phys., 12(24), 12277–12292, doi:10.5194/acp-12-12277-2012, 2012.

Fan, J. and Zhang, R.: Atmospheric oxidation mechanism of isoprene, Environ. Chem., 1(3), 140–149, doi:10.1071/EN04045, 2004.

10 Fantechi, G., Jensen, N. R., Saastad, O., Hjorth, J. and Peeters, J.: Reactions of Cl atoms with selected VOCs: Kinetics, products and mechanisms, J. Atmos. Chem., 31(3), 247–267, doi:10.1023/A:1006033910014, 1998.

Faxon, C., Bean, J. and Ruiz, L.: Inland Concentrations of Cl2 and ClNO2 in Southeast Texas Suggest Chlorine Chemistry Significantly Contributes to Atmospheric Reactivity, Atmosphere (Basel)., 6(10), 1487–1506, doi:10.3390/atmos6101487, 2015.

15 Faxon, C. B. and Allen, D. T.: Chlorine chemistry in urban atmospheres: A review, Environ. Chem., 10(3), 221–233, doi:10.1071/EN13026, 2013.

Goldstein, A. H. and Galbally, I. E.: Known and unexplored organic constituents in the earth's atmosphere, Environ. Sci. Technol., 41(5), 1514–1521, doi:10.1021/es072476p, 2007.

de Gouw, J. and Warneke, C.: Measurements of volatile organic compounds in the earth's atmosphere using proton-transfer-
20 reaction mass spectrometry, Mass Spectrom. Rev., 26(2), 223–257, doi:10.1002/mas.20119, 2007.

Griffin, R. J., Cocker, D. R. and Seinfeld, J. H.: Incremental aerosol reactivity: Application to aromatic and biogenic hydrocarbons, Environ. Sci. Technol., 33(14), 2403–2408, doi:10.1021/es981330a, 1999.

Guenther, a., Karl, T., Harley, P., Wiedinmyer, C., Palmer, P. I. and Geron, C.: Estimates of global terrestrial isoprene emissions using MEGAN (Model of Emissions of Gases and Aerosols from Nature), Atmos. Chem. Phys., 6(11), 3181–
25 3210, doi:10.5194/acpd-6-107-2006, 2006.

Guenther, A. B., Jiang, X., Heald, C. L., Sakulyanontvittaya, T., Duhl, T., Emmons, L. K. and Wang, X.: The model of emissions of gases and aerosols from nature version 2.1 (MEGAN2.1): An extended and updated framework for modeling biogenic emissions, Geosci. Model Dev., 5(6), 1471–1492, doi:10.5194/gmd-5-1471-2012, 2012.

Hawley, B., McKenna, D., Marchese, A. and Volckens, J.: Time course of bronchial cell inflammation following exposure to
30 diesel particulate matter using a modified EAVES, Toxicol. Vitr., 28(5), 829–837, doi:10.1016/j.tiv.2014.03.001, 2014.

Heald, C. L., Kroll, J. H., Jimenez, J. L., Docherty, K. S., Decarlo, P. F., Aiken, A. C., Chen, Q., Martin, S. T., Farmer, D. K. and Artaxo, P.: A simplified description of the evolution of organic aerosol composition in the atmosphere, Geophys. Res. Lett., 37(8), doi:10.1029/2010GL042737, 2010.

Hildebrandt, L., Donahue, N. M. and Pandis, S. N.: High formation of secondary organic aerosol from the photo-oxidation of

toluene, Atmos. Chem. Phys., 9(9), 2973–2986, doi:10.5194/acp-9-2973-2009, 2009.

Huang, M., Zhang, W., Gu, X., Hu, C., Zhao, W., Wang, Z. and Fang, L.: Size distribution and chemical composition of secondary organic aerosol formed from Cl-initiated oxidation of toluene, J. Environ. Sci., 24(5), 860–864, doi:10.1016/S1001-0742(11)60840-1, 2012.

5 Huang, M., Liu, X., Hu, C., Guo, X., Gu, X., Zhao, W., Wang, Z., Fang, L. and Zhang, W.: Aerosol laser time-of-flight mass spectrometer for the on-line measurement of secondary organic aerosol in smog chamber, Meas. J. Int. Meas. Confed., 55(3), 394–401, doi:10.1016/j.measurement.2014.05.038, 2014.

Jimenez, J. L., Canagaratna, M. R., Donahue, N. M., Prevot, a. S. H., Zhang, Q., Kroll, J. H., DeCarlo, P. F., Allan, J. D., Coe, H., Ng, N. L., Aiken, a. C., Docherty, K. S., Ulbrich, I. M., Grieshop, A. P., Robinson, a. L., Duplissy, J., Smith, J. D.,
10 Wilson, K. R., Lanz, V. a., Hueglin, C., Sun, Y. L., Tian, J., Laaksonen, A., Raatikainen, T., Rautiainen, J., Vaattovaara, P., Ehn, M., Kulmala, M., Tomlinson, J. M., Collins, D. R., Cubison, M. J., Dunlea, J., Huffman, J. A., Onasch, T. B., Alfarra, M. R., Williams, P. I., Bower, K., Kondo, Y., Schneider, J., Drewnick, F., Borrmann, S., Weimer, S., Demerjian, K., Salcedo, D., Cottrell, L., Griffin, R., Takami, A., Miyoshi, T., Hatakeyama, S., Shimono, A., Sun, J. Y., Zhang, Y. M., Dzepina, K., Kimmel, J. R., Sueper, D., Jayne, J. T., Herndon, S. C., Trimborn, a. M., Williams, L. R., Wood, E. C.,
15 Middlebrook, A. M., Kolb, C. E., Baltensperger, U. and Worsnop, D. R.: Evolution of Organic Aerosols in the Atmosphere, Science (80-.)., 326(5959), 1525–1529, doi:10.1126/science.1180353, 2009.

Kamilli, K. A., Ofner, J., Lendl, B., Schmitt-Kopplin, P. and Held, A.: New particle formation above a simulated salt lake in aerosol chamber experiments, Environ. Chem., 12(4), 489–503, doi:10.1071/EN14225, 2015.

Kanakidou, M., Seinfeld, J. H., Pandis, S. N., Barnes, I., Dentener, F. J., Facchini, M. C., Van Dingenen, R., Ervens, B., Nenes,
20 A., Nielsen, C. J., Swietlicki, E., Putaud, J. P., Balkanski, Y., Fuzzi, S., Horth, J., Moortgat, G. K., Winterhalter, R., Myhre, C. E. L., Tsigaridis, K., Vignati, E., Stephanou, E. G. and Wilson, J.: Organic aerosol and global climate modelling: a review, Atmos. Chem. Phys., 5(4), 1053–1123, doi:10.5194/acp-5-1053-2005, 2005.

Karlsson, R. S., Szente, J. J., Ball, J. C. and Maricq, M. M.: Homogeneous aerosol formation by the chlorine atom initiated oxidation of toluene, J. Phys. Chem. A, 105(1), 82–96, doi:10.1021/jp001831u, 2001.

25 Kokkola, H., Yli-Pirila, P., Vesterinen, M., Korhonen, H., Keskinen, H., Romakkaniemi, S., Hao, L., Kortelainen, A., Joutsensaari, J., Worsnop, D. R., Virtanen, A. and Lehtinen, K. E. J.: The role of low volatile organics on secondary organic aerosol formation, Atmos. Chem. Phys., 14(3), 1689–1700, doi:10.5194/acp-14-1689-2014, 2014.

Koo, B., Knipping, E. and Yarwood, G.: 1.5-Dimensional volatility basis set approach for modeling organic aerosol in CAMx and CMAQ, Atmos. Environ., 95, 158–164, doi:10.1016/j.atmosenv.2014.06.031, 2014.

30 Krechmer, J. E., Pagonis, D., Ziemann, P. J. and Jimenez, J. L. L.: Quantification of gas-wall partitioning in Teflon environmental chambers using rapid bursts of low-volatility oxidized species generated in-situ, Environ. Sci. Technol., acs.est.6b00606, doi:10.1021/acs.est.6b00606, 2016.

Kroll, J. H., Ng, N. L., Murphy, S. M., Flagan, R. C. and Seinfeld, J. H.: Secondary organic aerosol formation from isoprene photooxidation., Environ. Sci. Technol., 40(6), 1869–1877, doi:10.1021/es0524301, 2006.

Kroll, J. H., Chan, A. W. H., Ng, N. L., Flagan, R. C. and Seinfeld, J. H.: Reactions of semivolatile organics and their effects on secondary organic aerosol formation, Environ. Sci. Technol., 41(10), 3545–3550, doi:10.1021/es062059x, 2007.

Kroll, J. H., Donahue, N. M., Jimenez, J. L., Kessler, S. H., Canagaratna, M. R., Wilson, K. R., Altieri, K. E., Mazzoleni, L. R., Wozniak, A. S., Bluhm, H., Mysak, E. R., Smith, J. D., Kolb, C. E. and Worsnop, D. R.: Carbon oxidation state as a

5   metric for describing the chemistry of atmospheric organic aerosol., Nat. Chem., 3(2), 133–139, doi:10.1038/nchem.948, 2011.

Kwan, A. J., Chan, A. W. H., Ng, N. L., Kjaergaard, H. G., Seinfeld, J. H. and Wennberg, P. O.: Peroxy radical chemistry and OH radical production during the NO 3-initiated oxidation of isoprene, Atmos. Chem. Phys., 12(16), 7499–7515, doi:10.5194/acp-12-7499-2012, 2012.

10   Lee, B. H., Lopez-Hilfiker, F. D., Mohr, C., Kurtén, T., Worsnop, D. R. and Thornton, J. A.: An iodide-adduct high-resolution time-of-flight chemical-ionization mass spectrometer: Application to atmospheric inorganic and organic compounds, Environ. Sci. Technol., 48(11), 6309–6317, doi:10.1021/es500362a, 2014.

Lei, W. and Zhang, R.: Chlorine atom addition reaction to isoprene: a theoretical study, J. Chem. Phys., 113(1), 153–157, doi:10.1063/1.481782, 2000.

15   Lewandowski, M., Jaoui, M., Offenberg, J. H., Krug, J. D. and Kleindienst, T. E.: Atmospheric oxidation of isoprene and 1,3-butadiene: Influence of aerosol acidity and relative humidity on secondary organic aerosol, Atmos. Chem. Phys., 15(7), 3773–3783, doi:10.5194/acp-15-3773-2015, 2015.

Lin, Y. H., Zhang, Z., Docherty, K. S., Zhang, H., Budisulistiorini, S. H., Rubitschun, C. L., Shaw, S. L., Knipping, E. M., Edgerton, E. S., Kleindienst, T. E., Gold, A. and Surratt, J. D.: Isoprene epoxydiols as precursors to secondary organic

20   aerosol formation: Acid-catalyzed reactive uptake studies with authentic compounds, Environ. Sci. Technol., 46(1), 250–258, doi:10.1021/es202554c, 2012.

Liu, J., D'Ambro, E. L., Lee, B. H., Lopez-Hilfiker, F. D., Zaveri, R. A., Rivera-Rios, J. C., Keutsch, F. N., Iyer, S., Kurten, T., Zhang, Z., Gold, A., Surratt, J. D., Shilling, J. E. and Thornton, J. A.: Efficient Isoprene Secondary Organic Aerosol Formation from a Non-IEPOX Pathway, Environ. Sci. Technol., 50(18), 9872–9880, doi:10.1021/acs.est.6b01872, 2016.

25   Loza, C. L., Chan, A. W. H., Galloway, M. M., Keutsch, F. N., Flagan, R. C. and Seinfeld, J. H.: Characterization of vapor wall loss in laboratory chambers, Environ. Sci. Technol., 44(13), 5074–5078, doi:10.1021/es100727v, 2010.

Matsunaga, A. and Ziemann, P. J.: Yields of beta-hydroxynitrates, dihydroxynitrates, and trihydroxynitrates formed from OH radical-initiated reactions of 2-methyl-1-alkenes., Proc. Natl. Acad. Sci. U. S. A., 107(15), 6664–6669, doi:10.1073/pnas.0910585107, 2010.

30   Murphy, B. N., Donahue, N. M., Fountoukis, C., Dall'Osto, M., O'Dowd, C., Kiendler-Scharr, A. and Pandis, S. N.: Functionalization and fragmentation during ambient organic aerosol aging: Application of the 2-D volatility basis set to field studies, Atmos. Chem. Phys., 12(22), 10797–10816, doi:10.5194/acp-12-10797-2012, 2012.

Ng, N. L., Kroll, J. H., Chan, a W. H., Chhabra, P. S., Flagan, R. C. and Seinfeld, J. H.: Secondary organic aerosol formation from m-xylene, toluene, and benzene, Atmos. Chem. Phys., 7(14), 3909–3922, doi:10.5194/acp-7-3909-2007, 2007.

Ng, N. L., Canagaratna, M. R., Zhang, Q., Jimenez, J. L., Tian, J., Ulbrich, I. M., Kroll, J. H., Docherty, K. S., Chhabra, P. S., Bahreini, R., Murphy, S. M., Seinfeld, J. H., Hildebrandt, L., Donahue, N. M., Decarlo, P. F., Lanz, V. A., Prévôt, A. S. H., Dinar, E., Rudich, Y. and Worsnop, D. R.: Organic aerosol components observed in Northern Hemispheric datasets from Aerosol Mass Spectrometry, Atmos. Chem. Phys., 10(10), 4625–4641, doi:10.5194/acp-10-4625-2010, 2010.

Ng, N. L., Herndon, S. C., Trimborn, a., Canagaratna, M. R., Croteau, P. L., Onasch, T. B., Sueper, D., Worsnop, D. R., Zhang, Q., Sun, Y. L. and Jayne, J. T.: An Aerosol Chemical Speciation Monitor (ACSM) for Routine Monitoring of the Composition and Mass Concentrations of Ambient Aerosol, Aerosol Sci. Technol., 45(7), 780–794, doi:10.1080/02786826.2011.560211, 2011.

Nguyen, T. B., Coggon, M. M., Bates, K. H., Zhang, X., Schwantes, R. H., Schilling, K. A., Loza, C. L., Flagan, R. C., Wennberg, P. O. and Seinfeld, J. H.: Organic aerosol formation from the reactive uptake of isoprene epoxydiols (IEPOX) onto non-acidified inorganic seeds, Atmos. Chem. Phys., 14(7), 3497–3510, doi:10.5194/acp-14-3497-2014, 2014.

Nordmeyer, T., Wang, W., Ragains, M. L., Finlayson-Pitts, B. J., Spicer, C. W. and Plastridge, R. A.: Unique products of the reaction of isoprene with atomic chlorine: Potential markers of chlorine atom chemistry, Geophys. Res. Lett., 24(13), 1615–1618, doi:10.1029/97GL01547, 1997.

Odum Jay, R., Hoffmann, T., Bowman, F., Collins, D., Flagan Richard, C. and Seinfeld John, H.: Gas particle partitioning and secondary organic aerosol yields, Environ. Sci. Technol., 30(8), 2580–2585, doi:10.1021/es950943+, 1996.

Ofner, J., Balzer, N., Buxmann, J., Grothe, H., Schmitt-Kopplin, P., Platt, U. and Zetzsch, C.: Halogenation processes of secondary organic aerosol and implications on halogen release mechanisms, Atmos. Chem. Phys., 12(13), 5787–5806, doi:10.5194/acp-12-5787-2012, 2012.

Ofner, J., Kamilli, K. A., Held, A., Lendl, B. and Zetzsch, C.: Halogen-induced organic aerosol (XOA): a study on ultra-fine particle formation and time-resolved chemical characterization, Faraday Discuss., 165, 115–135, doi:10.1039/c3fd00093a, 2013.

Orlando, J. J., Tyndall, G. S., Apel, E. C., Riemer, D. D. and Paulson, S. E.: Rate coefficients and mechanisms of the reaction of Cl-atoms with a series of unsaturated hydrocarbons under atmospheric conditions, Int. J. Chem. Kinet., 35(8), 334–353, doi:10.1002/kin.10135, 2003.

Pankow, J. F.: An absorption model of gas/particle partitioning of organic compounds in the atmosphere, Atmos. Environ., 28(2), 185–188, doi:10.1016/1352-2310(94)90093-0, 1994.

Pathak, R. K., Presto, A. A., Lane, T. E., Stanier, C. O., Donahue, N. M. and Pandis, S. N.: Ozonolysis of α-pinene: parameterization of secondary organic aerosol mass fraction, Atmos. Chem. Phys., 7(14), 3811–3821, doi:10.5194/acp-7-3811-2007, 2007.

Paulot, F., Crounse, J. D., Kjaergaard, H. G., Kroll, J. H., Seinfeld, J. H. and Wennberg, P. O.: Isoprene photooxidation: new insights into the production of acids and organic nitrates, Atmos. Chem. Phys., 9(4), 1479–1501, doi:10.5194/acp-9-1479-2009, 2009.

Pierce, J. R., Engelhart, G. J., Hildebrandt, L., Weitkamp, E. a., Pathak, R. K., Donahue, N. M., Robinson, a. L., Adams, P. J.

and Pandis, S. N.: Constraining Particle Evolution from Wall Losses, Coagulation, and Condensation-Evaporation in Smog-Chamber Experiments: Optimal Estimation Based on Size Distribution Measurements, Aerosol Sci. Technol., 42(12), 1001–1015, doi:10.1080/02786820802389251, 2008.

Pope, C. A., Dockery, D. W., Chow, J. C., Watson, J. G., Mauderly, J. L., Costa, D. L., Wyzga, R. E., Vedal, S., Hidy, G. M., Altshuler, S. L., Marrack, D., Heuss, J. M., Wolff, G. T. and Arden Pope III, C.: Health Effects of Fine Particulate Air Pollution: Lines that Connect, J. Air Waste Manage. Assoc., 56(6), 1368–1380, doi:10.1080/10473289.2006.10464485, 2006.

Ragains, M. L. and FinlaysonPitts, B. J.: Kinetics and mechanism of the reaction of Cl atoms with 2-methyl-1,3-butadiene (isoprene) at 298 K, J. Phys. Chem. A, 101(8), 1509–1517, doi:10.1021/jp962786m, 1997.

Riedel, T. P., Bertram, T. H., Crisp, T. A., Williams, E. J., Lerner, B. M., Vlasenko, A., Li, S. M., Gilman, J., De Gouw, J., Bon, D. M., Wagner, N. L., Brown, S. S. and Thornton, J. A.: Nitryl chloride and molecular chlorine in the coastal marine boundary layer, Environ. Sci. Technol., 46(19), 10463–10470, doi:10.1021/es204632r, 2012.

Riemer, D. D., Apel, E. C., Orlando, J. J., Tyndall, G. S., Brune, W. H., Williams, E. J., Lonneman, W. A. and Neece, J. D.: Unique isoprene oxidation products demonstrate chlorine atom chemistry occurs in the Houston, Texas urban area, J. Atmos. Chem., 61(3), 227–242, doi:10.1007/s10874-009-9134-5, 2008.

Riva, M., Healy, R. M., Flaud, P. M., Perraudin, E., Wenger, J. C. and Villenave, E.: Gas- and Particle-Phase Products from the Chlorine-Initiated Oxidation of Polycyclic Aromatic Hydrocarbons, J. Phys. Chem. A, 119(45), 11170–11181, doi:10.1021/acs.jpca.5b04610, 2015.

Schwantes, R. H., Teng, A. P., Nguyen, T. B., Coggon, M. M., Crounse, J. D., St. Clair, J. M., Zhang, X., Schilling, K. A., Seinfeld, J. H. and Wennberg, P. O.: Isoprene NO$_3$ Oxidation Products from the RO$_2$ + HO$_2$ Pathway, J. Phys. Chem. A, 119(40), 10158–10171, doi:10.1021/acs.jpca.5b06355, 2015.

Surratt, J. D., Murphy, S. M., Kroll, J. H., Ng, N. L., Hildebrandt, L., Sorooshian, A., Szmigielski, R., Vermeylen, R., Maenhaut, W., Claeys, M., Flagan, R. C. and Seinfeld, J. H.: Chemical composition of secondary organic aerosol formed from the photooxidation of isoprene, J. Phys. Chem. A, 110(31), 9665–9690, doi:10.1021/jp061734m, 2006.

Surratt, J. D., Chan, A. W., Eddingsaas, N. C., Chan, M., Loza, C. L., Kwan, A. J., Hersey, S. P., Flagan, R. C., Wennberg, P. O. and Seinfeld, J. H.: Reactive intermediates revealed in secondary organic aerosol formation from isoprene, Proc Natl Acad Sci U S A, 107(15), 6640–6645, doi:10.1073/pnas.0911114107, 2010.

Tanaka, P. L. and Allen, D. T.: Incorporation of Chlorine Reactions into the Carbon Bond-IV Mechanism (supplement), [online] Available from: http://www.utexas.edu/research/ceer/airquality/Chlorine Emissions.pdf, 2001.

Tanaka, P. L., Riemer, D. D., Chang, S., Yarwood, G., McDonald-Buller, E. C., Apel, E. C., Orlando, J. J., Silva, P. J., Jimenez, J. L., Canagaratna, M. R., Neece, J. D., Mullins, C. B. and Allen, D. T.: Direct evidence for chlorine-enhanced urban ozone formation in Houston, Texas, Atmos. Environ., 37(9-10), 1393–1400, doi:10.1016/S1352-2310(02)01007-5, 2003.

Thornton, J. A., Kercher, J. P., Riedel, T. P., Wagner, N. L., Cozic, J., Holloway, J. S., Dubé, W. P., Wolfe, G. M., Quinn, P. K., Middlebrook, A. M., Alexander, B. and Brown, S. S.: A large atomic chlorine source inferred from mid-continental

reactive nitrogen chemistry., Nature, 464(7286), 271–4, doi:10.1038/nature08905, 2010.

Verheggen, B. and Mozurkewich, M.: An inverse modeling procedure to determine particle growth and nucleation rates from measured aerosol size distributions, Atmos. Chem. Phys. Discuss., 6(2), 1679–1723, doi:10.5194/acp-6-2927-2006, 2006.

Wang, L., Arey, J. and Atkinson, R.: Reactions of chlorine atoms with a series of aromatic hydrocarbons, Environ. Sci. Technol., 39(14), 5302–5310, doi:10.1021/es0479437, 2005.

Xu, L., Kollman, M. S., Song, C., Shilling, J. E. and Ng, N. L.: Effects of NOx on the volatility of secondary organic aerosol from isoprene photooxidation, Environ. Sci. Technol., 48(4), 2253–2262, doi:10.1021/es404842g, 2014.

Yatavelli, R. L. N., Lopez-Hilfiker, F., Wargo, J. D., Kimmel, J. R., Cubison, M. J., Bertram, T. H., Jimenez, J. L., Gonin, M., Worsnop, D. R. and Thornton, J. a.: A Chemical Ionization High-Resolution Time-of-Flight Mass Spectrometer Coupled to a Micro Orifice Volatilization Impactor (MOVI-HRToF-CIMS) for Analysis of Gas and Particle-Phase Organic Species, Aerosol Sci. Technol., 46(February 2015), 1313–1327, doi:10.1080/02786826.2012.712236, 2012.

Young, C. J., Washenfelder, R. A., Edwards, P. M., Parrish, D. D., Gilman, J. B., Kuster, W. C., Mielke, L. H., Osthoff, H. D., Tsai, C., Pikelnaya, O., Stutz, J., Veres, P. R., Roberts, J. M., Griffith, S., Dusanter, S., Stevens, P. S., Flynn, J., Grossberg, N., Lefer, B., Holloway, J. S., Peischl, J., Ryerson, T. B., Atlas, E. L., Blake, D. R. and Brown, S. S.: Chlorine as a primary radical: Evaluation of methods to understand its role in initiation of oxidative cycles, Atmos. Chem. Phys., 14(7), 3427–3440, doi:10.5194/acp-14-3427-2014, 2014.

Zhang, X., Schwantes, R. H., McVay, R. C., Lignell, H., Coggon, M. M., Flagan, R. C. and Seinfeld, J. H.: Vapor wall deposition in Teflon chambers, Atmos. Chem. Phys., 15(8), 4197–4214, doi:10.5194/acp-15-4197-2015, 2015.

Zhao, B., Wang, S., Donahue, N. M., Chuang, W., Hildebrandt Ruiz, L., Ng, N. L., Wang, Y. and Hao, J.: Evaluation of one-dimensional and two-dimensional volatility basis sets in simulating the aging of secondary organic aerosol with smog-chamber experiments, Environ. Sci. Technol., 49(4), 2245–2254, doi:10.1021/es5048914, 2015.

Table 1. Summary of Experimental Conditions and Results

Exp.[a]	Isoprene (ppb)[b]	Chlorine (ppb)[c]	VOC:Cl$_2$	Cl$_2$ Inj.[d]	Ini Seed SA (um^2 cm^{-3})[e]	Max OA (µg m^{-3})[f]	Yield
A1	24	40	0.59	Ini	1510	15	0.230
A2	40	88	0.45	Ini	905	32	0.289
A3	82	115	0.71	Ini	811	47	0.207
A4	120	177	0.68	Ini	1328	84	0.253
A5	160	231	0.69	Ini	1769	91	0.205
C1	40	94	0.42	Cont	947	10	0.092
C2	120	180	0.67	Cont	881	37	0.111
C3	240	272	0.88	Cont	774	64	0.096
C4	300	246	1.22	Cont	1431	67	0.080
C5[g]	72	122	0.59	Cont	N/A	N/A	N/A
H1	180	359	0.50	Ini	775	180	0.360
H2[h]	244	681	0.48	Ini	1047	N/A	N/A

[a] "A": Initial chlorine injection experiments. "C": Continuous chlorine injection experiments. "H": High aerosol loading (>100 µg m^{-3}) initial chlorine injection experiments. Q-ACSM scan speed for Exp. H1 (500 ms amu^{-1}) was different from other experiments (200 ms amu^{-1})

[b] Initial isoprene concentration

[c] Amount of chlorine injected initially (for A1–A5 and H1–H2) or cumulative chlorine injected (for C1–C5)

[d] Chlorine injection method. "Ini" for initial injection; "Cont" for continuous chlorine injection

[e] Total initial surface area of ammonium sulfate seed aerosol

[f] Highest, particle wall-loss-corrected OA concentration observed

[g] No SEMS data available

[h] UV was turned off at T = 5 mins, see section S4
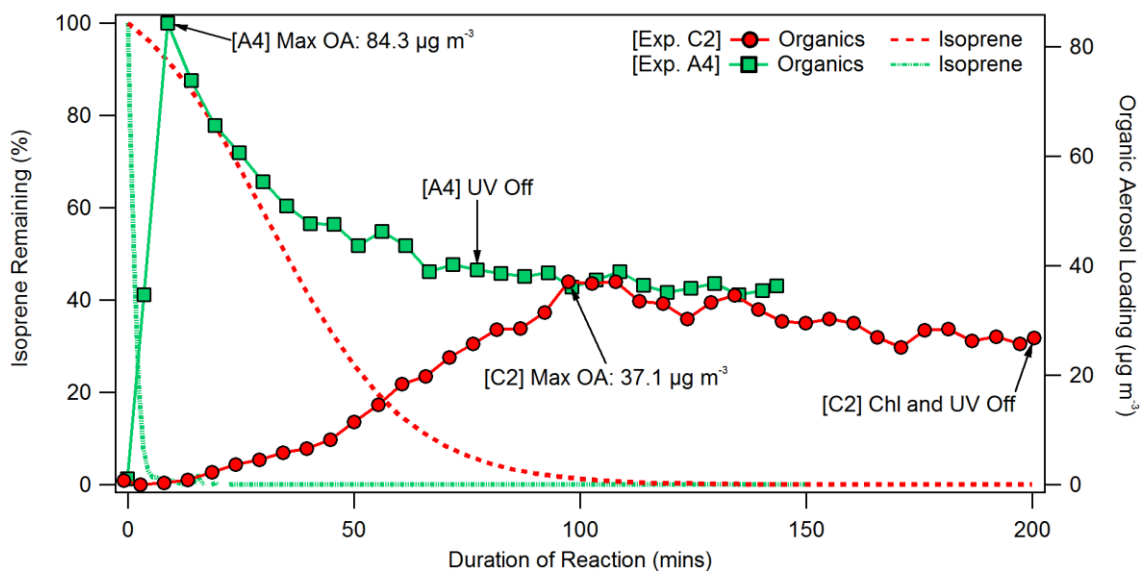
Figure 1: Comparison of SOA formation during continuous (C2) and initial (A4) chlorine injection experiments with similar precursor concentrations. SOA concentration is wall-loss corrected and averaged over five-minute intervals. Isoprene concentration is tracked using [H$_2$O]$_n$H$_3$O$^+$ CIMS and averaged over one-minute intervals.
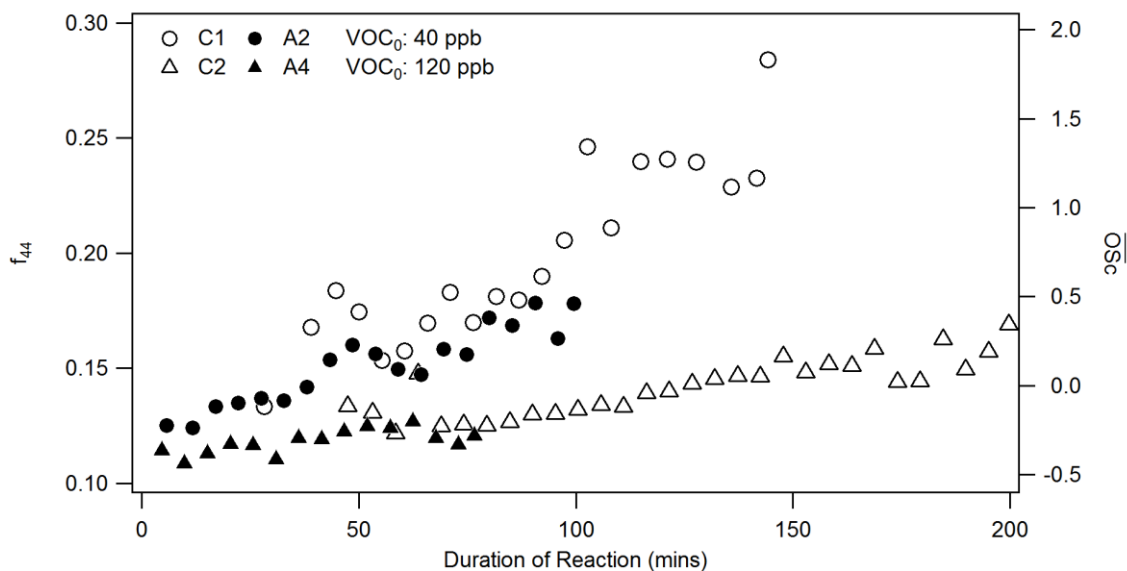
Figure 2: Comparison of SOA aging between two pairs (C1 and A2; C2 and A4) of initial and continuous chlorine injection experiments. The trend of f_{44} is consistent for each pair, regardless of chlorine injection method used. Higher initial isoprene concentration resulted in less oxidized organic aerosol (lower f_{44}). $\overline{OS}_C$ is estimated based on f_{44} (see section S2).
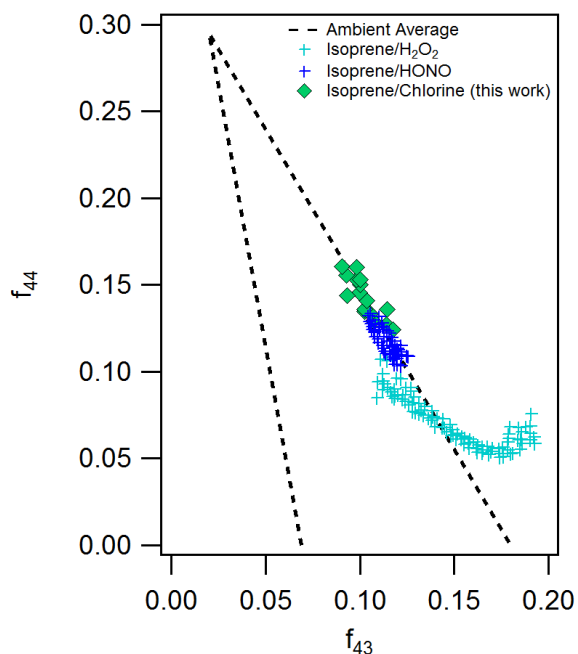
Figure 3: Oxidation state of SOA generated from chlorine-initiated oxidation (Exp. C3, five-minute averages) compared to OH-oxidation of isoprene under low- and high-NO$_x$ (Chhabra et al., 2011). Area enclosed by the dashed lines represent typical ambient OA measurements (Ng et al., 2010).
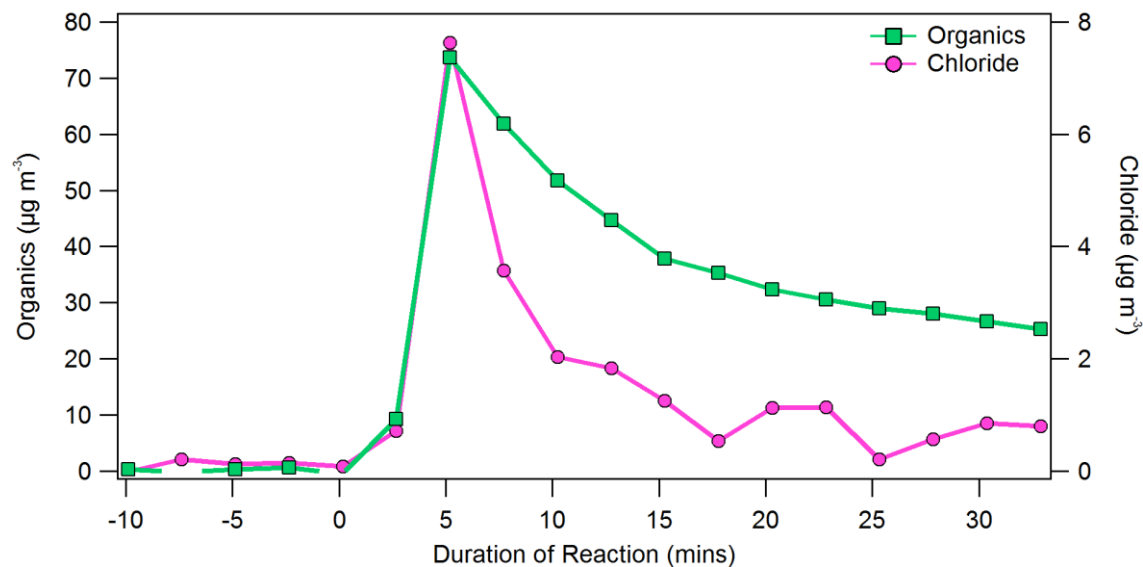
Figure 4: The raw organics and chloride measurements for Exp. H1. UV was turned on at T = 0. Apparent chloride concentration rapidly decreased to near-background levels while significant suspended OA mass remained. This rapid decrease is likely a measurement artifact due to build-up of chloride on the vaporizer surface, see section 3.2 and S4.
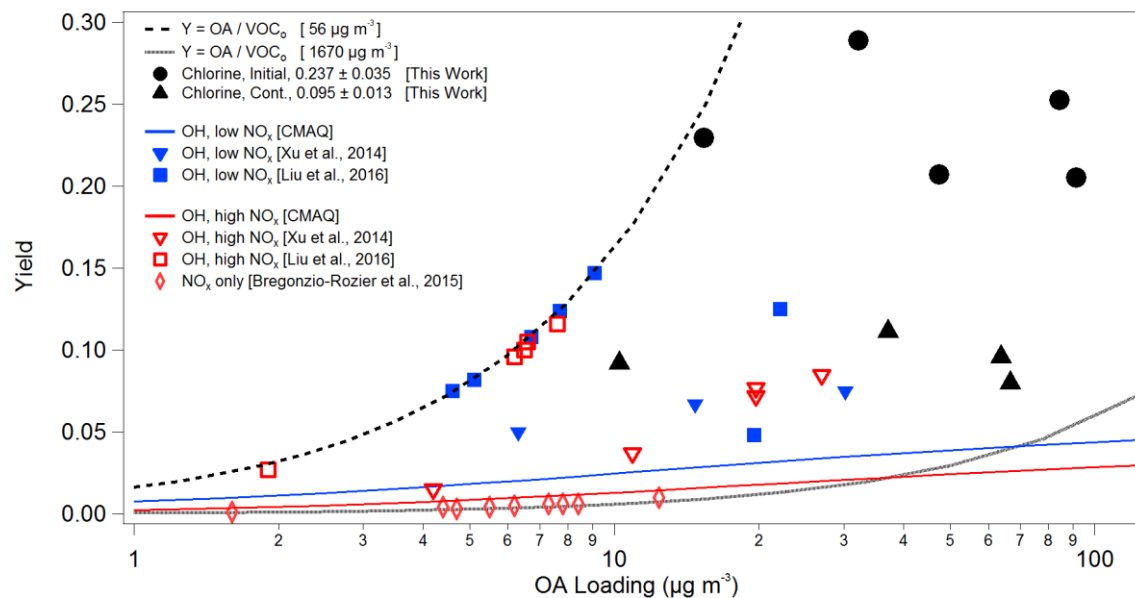
Figure 5: Comparison of observed isoprene-chlorine SOA yield with recent literature values (Brégonzio-Rozier et al., 2015; Liu et al., 2016; Xu et al., 2014). Dashed lines illustrate the concept of a "pre-defined" yield curve as discussed in the text. The yield used in CMAQ was reproduced using cited VBS parameters (Koo et al., 2014).
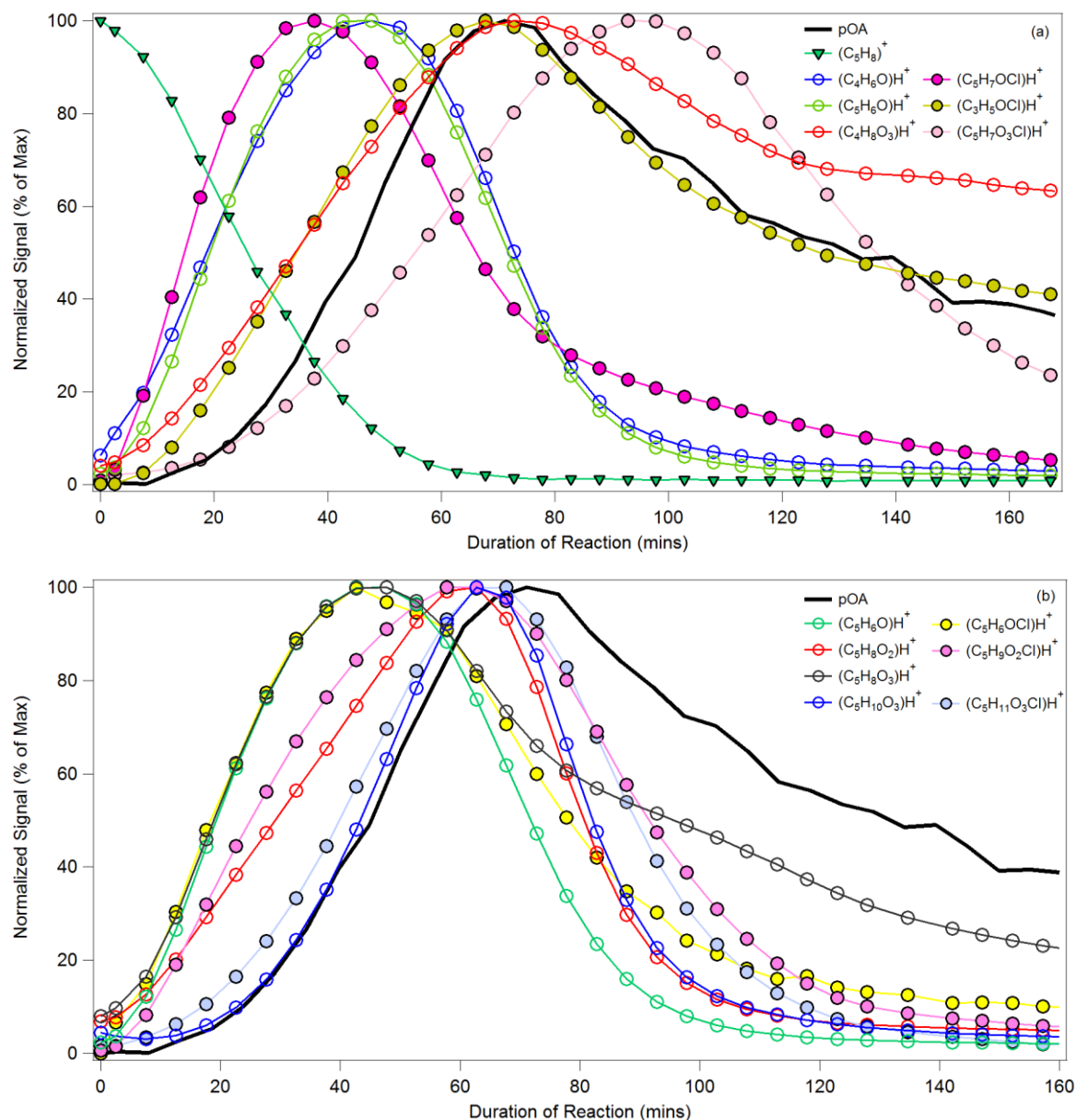
Figure 6: Observation of select gas-phase species using $(H_2O)_nH_3O^+$-CIMS plotted alongside SOA concentration for Exp. C5. Suspended particle concentration is shown. Ion signal for each individual species was normalized to its maximum value. Five minute averages are shown (a) Isoprene was completely depleted by the time maximum OA concentration was reached; multi-generational oxidation and chlorinate were clearly observed. (b) Observation of ions potentially resembling IEPOX, or $C_5H_{10}O_3$. Potential oxidation product ion $(C_5H_8O_3)H^+$ and interfering ions, $(C_5H_8O_2)H^+$ and $(C_5H_{11}O_3Cl)H^+$ are also shown.
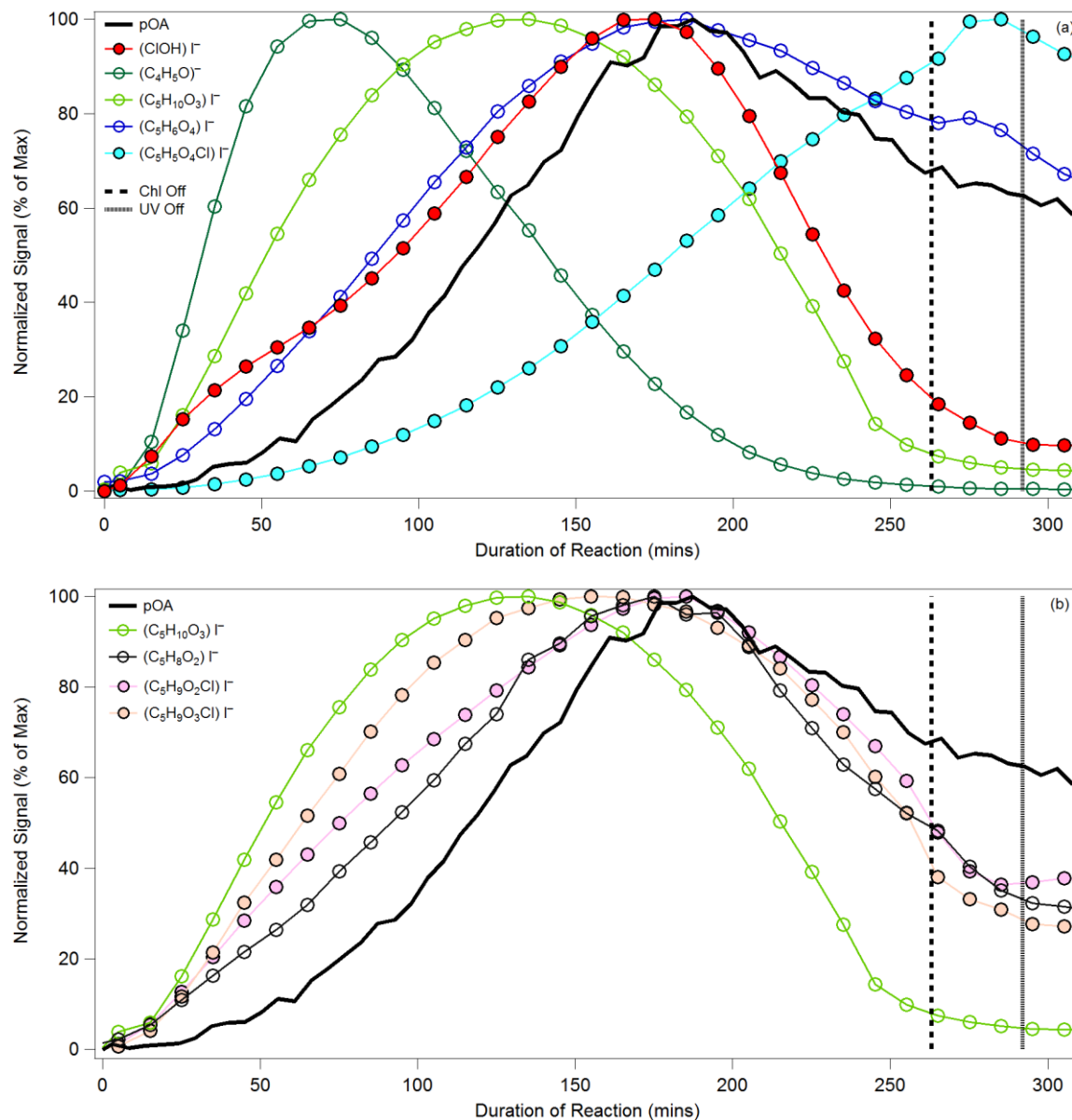
Figure 7: Observation of select gas-phase products using $(H_2O)I^-$ CIMS from Exp. C3. Chlorine injection stopped at T = 263 mins and UV lights were turned off at T = 292 mins. Ten-minute averages of normalized CIMS ion signals and five-minute averages of normalized, suspended OA concentrations are shown. Note that Exp. C3 (Fig. 7) and Exp. C5 (Fig. 6) have different precursor concentrations, hence the difference in the time required to achieve maximum OA concentration. (a) Multi-generational oxidation accompanying SOA formation; ClOH trend suggests OH radical production from isoprene oxidation (b) Observation of ions consistent with IEPOX; potential interfering ion trends were distinct from that of $(C_5H_8O_3)I^-$.